Slug Flow Characteristics and Their Effect on Corrosion Rates in Horizontal Oil and Gas Pipelines

Jyi-Yu Sun and W.P. Jepson, Ohio U.

SPE Members

II

ABSTRACT

The flow characteristics of slug flow and their effect on the corrosion rates are examined experimentally in a 100 mm diameter, horizontal, Plexiglass pipeline. The system was maintained at a pressure of 2 bars and temperature of approximately 35 °C. After initial tests with oil only and water only, 80% water and 20% oil, and 60% water and 40% oil mixtures were examined. Carbon dioxide was used as the gas. Using the stationary slugs described by Jepson[1,2], the mean wall shear stress and turbulent intensity at 7 different axial and three circumferential locations were measured using flush mounted TSI hot film anemometer probes. The regions included the film region ahead of the slug, the mixing zone at the slug front, and a short distance into the slug body. The oil, water, and carbon dioxide fractions were measured across a vertical diameter using a sampling probe. Corrosion rates at the top and bottom of the pipe were measured using electrical resistance probes. Pressure gradients across the slug front were also taken.

The results clearly show that the slug front is a highly turbulent region that has large wall shear stresses at the bottom of the pipe. The wall shear stress decreases with circumferential position but increases with increasing oil fraction in the fluids. For a Froude number of 12, the shear stress for water only is 26 N/m^2. For the mixture of 60% water and 40% oil a value of 97 N/m^2 is attained. These are much greater than anticipated. Instantaneous values are much larger than this. The corrosion rates are much greater than those predicted by usual laboratory methods, such as rotating cylinders or disks. The rates are shown to be greatest at the bottom of the pipe and correspond to the regions of high wall shear. Corrosion rates increase with an increase in oil concentration at the same Froude number. It is concluded that the wall shear stress associated with the slug front is sufficient to continuously remove corrosion products from the pipe wall.

References and illustrations at end of paper

INTRODUCTION

Internal corrosion of carbon-steel pipelines is a common problem in oil and gas production facilities which are designed for long-time operation. This problem has triggered the consideration of many corrosion control programs in various oil fields around the world. These methods include the selection of a pipe-wall thickness with sufficient corrosion allowance, the use of corrosion-resistant-alloy materials, the use of internally-coated pipe, dehydration of the oil-water mixture, and the corrosion-inhibitor injection. New pipeline design and service must consider corrosion control. Surface treatment such as injection of corrosion inhibitor into the flow system of pipelines is widely adopted. However, inability to predict accurately the flow regime in the multi-phase flow that would occur in the pipeline could seriously change the effectiveness of the inhibition process. By continuous injection or batch treatment commercial corrosion inhibitors can adsorb to the metal surface and form a barrier in the form of a protective film. This film can prevent further corrosion.

One of the crucial parameters in selecting an inhibitor is to know its effectiveness in service environments. A knowledge of the metal surface condition, operating temperature and pressure, fluid properties, solution pH and chemistry, and flow conditions, such as flow velocity and single- or multi-phase flows is necessary. Dissolved gas, especially oxygen and carbon dioxide, and fluid dynamics can drastically reduce the effectiveness of inhibitor[3].

The corrosion processes in oil and gas production pipelines involve the interaction between metal wall and the flowing fluids. Relative motion between the fluid and the metal surface will in general affect the rate of the corrosion. Ellison and Wen[4] have proposed a rational classification for flow effects on corrosion. Three different mechanisms, i.e. convective-mass-transfer-controlled corrosion, phase-transport-controlled corrosion, and

erosion-corrosion have been distinguished. For convective-mass-transfer-controlled corrosion, the corrosion rate is affected by either the convective transport of corrosive materials to the metal surface or the rate of dissolved corrosion products away from the surface. The phase-transport-controlled corrosion depends on the wetting of the metal surface by the phase containing corrosive material. The phase distribution is strongly affected by the multiphase flow. Erosion-Corrosion occurs when high velocity, high turbulence fluid flow and/or flow of abrasive materials prevents formation of protective film, allowing fresh material to be continuously exposed to the corrosive environment.

The multi-phase flow conditions in oil and gas pipelines are also important factors influencing the corrosion and the inhibitor effectiveness. A strong relationship has been found between field measurement of corrosion rate and flow regime[5].

Liquid and gas flowing simultaneously in a horizontal or a near horizontal pipe display a number of different interfacial multi-phase configurations which can be quantitatively shown in a flow regime map plotted according to the flow rates and fluid properties of the liquid and gas involved[6,7]. At low liquid flows a stratified or a stratified/wavy regime can exist. At a constant gas flow, an increase in the liquid velocity can change the flow from stratified to one of two "intermittent" patterns, i.e. either plug or slug flow. Plug flow is found at low gas velocities and consists of elongated gas bubbles that move through the liquid along the top of the pipe.

Slug flow always exists in long oil and gas pipelines when high oil and high gas production rates are required. Slug flow is similar to a stratified flow but with the intermittent appearance of high velocity liquid slugs which fill the whole pipe cross section and can be highly aerated. Slugs are formed when waves at the gas/liquid interface grow due to the drag from the faster moving gas flow. These waves bridge the pipe and are immediately accelerated to a velocity close to the gas velocity. Figure 1 shows an idealized slug unit which consists of four distinct zones: the stratified liquid film with gas pocket above it; the mixing zone; the slug body; and the slug tail. The fast moving slug of liquid (i.e. slug front) accelerates and scoops up the slow moving liquid film ahead of it into the mixing zone where an eddy is created. This highly turbulent mixing zone entrains gas which is passed back to form the slug body. After the passage of the slug, liquid is shed from the tail of the slug to a trailing film which moves slower than the slug body. This liquid mixes with more incoming liquid to form a film on which the next slug will propagate.

Experimental and theoretical verification of all the above zones has been performed by several researchers using different modeling approaches[8-10]. It was further suggested by Jepson[1] that slugs were hydraulic jumps propagating along a pipe. Experiments in a 10 cm diameter pipe were conducted on a 'stationary slug', i.e. a hydraulic jump, which is formed by forcing liquid under a gate. The 'slug' can be moved and made stationary at a fixed location by controlling the back pressure in the pipe. The front of a real moving slug moves with a translational velocity, V_t. The fluid in the slug body moves with a velocity, V_s, and the film before the front has a velocity, V_f. V_t is usually 1.2 to 1.3 times that of V_s. V_f is usually much smaller than V_t and V_s. The stationary jump has zero translational velocity and can be visualized as a slug where the frame of reference is taken as moving with the translational velocity of the slug.

Jepson[2] also reported the effect of the Froude number, calculated in the film ahead of the jump, on void fraction and

velocity profiles. It was also noted that the mixing vortex and the flow in the slug body for the stationary slugs and the true moving slugs are virtually identical. However, the measurements in a stationary slug are far easier to make than those in a fast moving, real slug, since the flow is not intermittent in the stationary case.

The study of corrosion/erosion and of the effectiveness of inhibitor film is usually conducted in the laboratory using single phase test systems[11]. The currently popular test method is to employ the "film persistence wheel test" in which the test cell containing coupons of pipe material and fluid is rotated on the wheel to provide agitation. Weight loss is compared between treated and untreated coupons under different test conditions, such as fluid temperature and salt concentration, etc.. However, this method does not consider the effect of flow mechanisms on the internal surface of the pipeline and, therefore, is believed to provide incorrect values for most multi-phase pipelines. Also the results from these tests are often extrapolated to large diameter pipelines. Great errors can occur in this process.

The existence of slug flow and its propagation in multi-phase oil and gas production pipelines can reduce the effectiveness of a corrosion inhibitor film due to the highly turbulent flow characteristics in the mixing zone. Jepson[2] and Sun[12] have shown that there are regions of high shearing forces which destroy the liquid boundary layer close to the wall. This makes the formation of a stable inhibitor film difficult. Further, it may be possible to strip off the film and corrosion material that is already present.

The exact mechanism for removing a corrosion inhibitor film from the pipe wall is still unclear. In order to understand the flow characteristics and to monitor the stability of the corrosion-inhibitor film, this work utilizes stationary slug flow to measure the oil, water, and gas fractions in the slug, the wall shear stress and turbulent intensity at 7 axial and 3 circumferential locations before and within the slug, pressure drops across the slug and within the slug, and corrosion/erosion rates at the bottom and the top of the pipe in the mixing zone.

EXPERIMENTAL SETUP

Simultaneous flow of oil, water, and gas in pipes is a common occurrence in mature oil and gas producing fields. The fluids are often transported together in a single pipeline to a central gathering station where the oil, water, and gas are separated. In recent years, the presence of carbon dioxide in these fluids is more frequent due to the occurrence of CO_2 gas production from deeper wells and also due to the use of enhanced oil recovery techniques involving CO_2 injection into the reservoir[13,14].

Carbon dioxide and free water react to form carbonic acid, which is corrosive to carbon steel pipes by forming corrosion products:

$$CO_2 + H_2O \rightarrow H_2CO_3 \text{, and}$$
$$Fe + H_2CO_3 \rightarrow FeCO_3 + H_2.$$
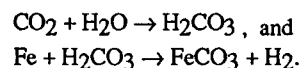
According to all these flow conditions in the oilfield, the experimental part is designed as following in order to understand the flow chanacteristcs when slugs present in the pipeline and their effect on corrosion/erosion of the steel pipes.

Selection of Liquids and Gas

Water and ARCO PAC 90 oil are the liquids used. Carbon dioxide is available from compressed gas cylinders. Water only, oil-water mixture of 20% oil and 80% water by volume, oil-water mixture of 40% oil and 60% water by volume, and oil only are selected as working fluid conditions.

Description of Flow Loop

The apparatus used is that developed by Jepson[1]. A 10.2 cm ID Plexiglass horizontal pipeline is employed with water, oil, and carbon dioxide as the working fluids. The schematic layout of the system is shown in Figure 2.

The oil and water are pumped from their respective tanks by centrifugal pumps into 7.6 cm ID PVC pipes. The flowrates are controlled by using a by-pass system for each liquid. Flowrates are measured in the 7.6 cm pipes by orifice plates and manometers. The flows are combined and passed into the 10.2 cm ID Plexiglass section where the mixture is forced under a gate G to form a fast moving liquid film. By measuring the wetted perimeter of the pipe that is contacted with liquid, the film depth, the mean velocity of the liquid film is calculated.

Carbon dioxide from compressed cylinders is forced into the system at location, J1, and at the top of water tank, J2. The carbon dioxide is first passed into an expansion tank and the flow rate is measured by a gas rotameter. The gas is also used to pressurize the system whose pressure is monitored by gauge B. It is released from valves I1 (fine control) and I2 (coarse control).

Downstream of gate G, a hydraulic jump (slug body) can form in the pipe. The jump can be maneuvered to the test section and made stationary there by controlling the gas flow into the pipeline at inlets, J1 and J2, and the back pressure by releasing gas from outlets, I1 and I2. The gas and liquids then flow into the water tank containing a specially designed de-entrainer table. The gas is released to the atmosphere and the oil and water are separated in the tank and then recirculated.

Using the film height and velocity before the jump, a very important parameter, the Froude number, Fr, before the jump can be calculated as

$$Fr = \frac{V_f}{\sqrt{g \times h_{eff}}} \quad \text{..} \quad (1)$$

where V_f, g, and h_{eff} are film velocity, acceleration due to gravity, and the effective height of the film, respectively. The effective height of the film is defined as the ratio of wetted area to the width of the liquid-gas interface in the film region ahead of the stationary slug.

Description of Test Section

The test section is illustrated in Figure 3. At position E, flush mounted hot film sensors are used to measure the mean wall shear stress and turbulent intensity of the flow near the wall at the bottom, side, and top of the pipe. Turbulent intensity is defined as the ratio of the standard deviation to the mean values of the wall shear stress data. The hot-film sensor employs a heat-transfer technique, which gives a correlation between wall shear stress and the heat transfer rate from the sensor to the fluid. Great care has to be taken to ensure that no gas pockets cover the probes for any prolonged periods of time, as this leads to burn-out of the probes. This is a particular problem at the top of the pipe at high flowrates. The voltage signal from each probe is passed to an IFA 100 anemometer system which converts these analog signals through an AD Converter and stores the data in digital form. The data is then processed using the Anemometry Software Package and a computer. By moving the slug to different axial locations, the wall shear can be measured at several points, before, at the front of, and, within the slug. The probes are initially calibrated and are recalibrated at regular periods and when there is any change of the fluid composition, such as the increase of oil concentration and the addition of corrosion inhibitor.

Corrosion/erosion rates are measured at the top and bottom of the pipe at locations, A, just downstream of the wall shear probes. Because of the large amount of gas being entrained in the water and oil-water mixture, linear polarization probes and other traditional methods cannot be utilized. An electrical resistance instrument with special probes is employed. The probe contains two elements, one is flush mounted on the metal surface, the other is beneath the surface without any contact with the surface. The latter wire serves as a reference element. The electrical resistance method relies on the fact that the DC ohmic resistance of an element will increase in inverse proportion to its cross-section. The progress of corrosion and its inhibition can therefore be monitored from changes in the electrical resistance of the element on the surface of a test probe by comparing with the reference wire[15]. Due to the high rates of corrosion, approximately three hours are needed for each measurement to ensure an adequate monitoring period. First hour is usually used to get thermal equilibrium of the E/R probes.

Several pressure tapings, locations denoted as D's, allow the pressure drops across and within the slug to be measured using differential U tube manometers. Fluid with a specific weight of 1.75 is used in the manometers.

A 6 mm diameter sampling probe C is used to withdraw fluid samples from the slug body within the test section. The probe can be positioned at any point across a vertical diameter. The sample is taken isokinetically and passed into a one-meter long tube with a fixed volume of 62.5 ml. Valves at each end of the tube are closed simultaneously and the flow is allowed to separate. The volumes of oil and water are measured using a graduated cylinder and then the volume of gas i.e. void fraction, α, is easily calculated.

Before any data are taken, a deoxygenation procedure is first used to ensure that the corrosion measurement is not affected by the existence of oxygen in the system. Since a hydraulic jump has the ability to entrain and mix with gas. Carbon dioxide in the system is used to purge out the oxygen. CHEMets Dissolved Oxygen Test Kits Models 0-40 and 0-100 are selected to monitor the oxygen concentration in the testing fluid. It is found that the oxygen concentration is greater than 100 ppb before and smaller than 10 ppb after the deoxygenation procedure.

Flow conditions at Froude numbers of 6, 9, and 12 for liquid films coming into the stationary slug were used for each fluid composition, i.e. water, oil, and oil-water mixtures. These values were chosen since they reflect various types of slugs that would generally exist in most flowlines. Channel flows at these Froude numbers can produce steady and strong hydraulic jumps, whose flow configurations are shown in Figure 4, as defined by Chow[16]. Although the figure presents hydraulic jumps in open channel, slug flows in circular pipes give similar profiles at the same Froude

numbers. This has been confirmed by Jepson[1,2] and Sun[12] through experimental measurements and observations. Flows at Froude numbers 6, 9, and 12 in this experimental setup can create highly turbulent eddies at the mixing zone of the jump.

Fluids of water only and oil only flowing in the system were first investigated to identify the slug flow characteristics of single-component (i.e. single-liquid) two-phase flow. These flow characteristics include liquid holdups, pressure drops across and within the slugs, wall shear stresses, turbulent intensities, and surface corrosion/erosion rates by the slug body. Oil-water mixtures, namely 20% oil and 80% water and 40% oil and 60% water by volume, were examined at the same Froude numbers as in the single-component flow system to investigate the effects of the addition of a third phase (i.e. oil phase in this study) on slug flow characteristics.

RESULTS AND DISCUSSION

Void Fraction (Gas Holdup)

The void fractions, α, and the liquid fractions, H_L, were obtained at three axial positions, that is the slug front, and at 25 and 50 cm into the slug body. For each position, five locations across a vertical diameter were selected to withdraw samples to measure local void fraction. These locations were 0.054, 0.225, 0.475, 0.725, and 0.947 pipe diameters from the bottom of the pipe.

For a given void fraction, liquid holdup, H_L, can be calculated as

$$H_L = 1 - \alpha \qquad (2)$$

At each location, four or five repeated measurements were taken to ensure the repeatability and precision of the isokinetic sample-taking technique.

The average void fractions of the slug body at each position were calculated from the five vertical local void fractions using Simpson's Rule.

An increase of Froude number increases the local and average void fractions for all the various fluid compositions. This can be seen in Figures 5, 6, and 7 for water only and water-oil mixtures of 80% water and 20% oil; and 60% water and 40% oil, respectively. Slug flows at higher Froude numbers have better ability to entrain gases because of more turbulent eddy motion in the mixing zone.

From Figures 5, 6, and 7, it is noticed in each case that the void fraction is always smaller at the bottom of the pipe than the top. It can also be seen that at a Froude number of 6, buoyancy forces act quickly in the relatively slow moving fluid in the slug body and the gas bubbles tend to move towards the top of the pipe.

Further, not all the gas that is entrained at the slug front is passed back, but gas bubbles burst and reenter the gas pocket in front of the slug. As the Froude number increases, the length of the zone, where the entrainment occurs, increases. This enhances the mixing process and more gas passes back into the slug body. Hence, a more homogeneous flow in the slug body is seen at higher Froude numbers. These conclusions can also be made from the calculated results of average void fractions at each axial position.

Other Froude numbers for the water-carbon dioxide system were also examined to study the effects of jump 'strength' on the void fraction at a position of 25 cm within the slug body. The comparison between the experimental data and the prediction from the correlation of Gregory et al.[17] is given in Figure 8. It can be seen that the correlation and the measured data show good agreement except at larger Froude numbers. Here, the effect of pipe size becomes significant since more gas can pass back to the back of a stationary slug for larger pipe at high Froude numbers. A similar correlation to that proposed by Gregory et al. can be drawn from these measured data with different values of the correlation constants. It can be written in the same way as

$$H_L = \frac{1}{1 + \left(\dfrac{V_M}{6.427} \right)^{1.816}} \qquad (3)$$

where V_M is the mixture velocity.

The comparison among Figures 5, 6, and 7 indicates the effect of the oil concentration on the amount of gas entrained at various locations within the slug body. Table 1 gives this two-component effect on void fraction at 25 cm within the slug body. It is clearly seen that increasing the oil concentration decreases the amount of gas entrained. A Froude number of 9, for water only, can produce a strong jump, but for the mixture of 40% oil and 60% water, it produces a weaker jump, since, as shown later, the vortex intensity (defined as turbulent intensity in this study) is clearly decreasing for increasing oil concentration. Further, there is less gas at the bottom of the pipe at the higher oil concentration. Most of the gas resides near the top of the pipe. The comparison between the measured data and both the correlations of present work and of Gregory et al.[17] also shows satisfactory agreement, except flows at low Froude numbers, where the existence of an oil phase as the second liquid phase becomes significant in affecting the ability of the slug front to entrain gas in the slug flow.

Measurements of the oil and water fractions were taken simultaneously with the gas fraction. It was found that the oil-water composition only changed by 1 or 2% across the pipe cross-section at Froude numbers of 9 and 12, and only by at most 4 or 5% at a Froude number of 6, at 25 and 50 cm within the slug body. This shows that the liquid phases were well mixed and homogeneous.

Mean Wall Shear Stress and Turbulent Intensity

Figures 9, 10, and 11 show the mean wall shear and associated turbulent intensity at the bottom of the pipe at locations at the front of and within the slugs for the cases of water only, and of oil-water mixtures of 20% oil and 80% water and of 40% oil and 60% water, respectively.

In each case, both the wall shear and the turbulent intensity increase substantially with an increase in Froude number. The largest changes occur at the highest Froude number. These changes occur within 25 to 50 cm from the slug front (this zone is usually characterized as the liquid-gas mixing zone for slug flow within conduits). This axial profile of wall shear stress is identical to the findings of Kvernvold et al.[18] and Jepson et al.[1]. Kvernold et al. used a Laser Doppler Velocimetry to measure the velocity distribution in a horizontal slug flow and concluded that a large change of velocity occurred in the mixing region of the slug. Jepson measured the cross-sectional velocity profiles in a stationary slug

(hydraulic jump) and found a large velocity gradient near the wall within the mixing zone of the slug body.

The mean wall shear stress for water only increases from a value of 7 N/m^2 at a Froude number of 6, to 13 N/m^2 at a Froude number of 9, and 26 N/m^2 at a Froude number of 12. Instantaneous values of the measured shear stress are as high as 37 N/m^2 at the highest Froude number. As the oil concentration is increased to 20% and then 40%, the mean wall shear stresses increase to 68 N/m^2 and 97 N/m^2 (with the instantaneous values of 98 N/m^2 and 171 N/m^2), respectively, at the Froude number of 12. Similar increases are shown at the lower Froude numbers.

The turbulent intensity also is shown to change rapidly at the slug front and some distance into the slug body. In each case, the turbulent intensity increases with Froude number. However, increasing oil concentration decreases the turbulent intensity at all Froude numbers. There is a subsequent decease in the ability of the slug front to entrain gas.

Figure 12 compares mean wall shear stress measurements at the bottom, side, and top of the pipe at the slug front at a Froude number of 6. The shear stress is greatest at the bottom and decreases substantially with circumferential position until a minimum is reached at the top of the pipe. This is probably due to more gas being present towards the upper half of the pipe.

The variation of turbulent intensity with circumferential position is more difficult to determine. This depends on the Froude numbers. At low Froude numbers the most intense mixing occurs toward the upper half of the pipe, whilst at high Froude numbers the mixing is apparent across the whole pipe.

It is clear that, as a slug passes down a pipe, there is associated with it a substantial change in both the wall shear stress and turbulence. This can have significant effects on the corrosion/erosion rate and also on the formation of the inhibitor film.

Pressure Drops across the Slug Front and within the Slug Body

The pressure difference between the fluid before the slug front and 30 and 60 cm within the slug were measured and the results are listed in Table 2. The first pressure drop, denoted P1 in this table, indicates the pressure drop across the slug front, and the second, denoted P2, is the pressure across both the slug front and the slug body. The pressure drop has been shown by Dukler and Hubbard[6] as a result of acceleration (deceleration in stationary slug) and friction losses. Knowing the liquid flow rate, the average velocity of the liquid film, and the liquid holdup in the liquid film or in the slug body, the pressure drop due to the acceleration of the liquid film, ΔP_a, can then be calculated using the following equation

$$\Delta P_a = \frac{x}{A}\left(V_s - V_{fe}\right) \quad\text{.......................................} \quad (4)$$

where x is the rate at which mass is picked up by the slug, V_s is mean velocity of fluid in the slug, and V_{fe} is the mean velocity of fluid in the film in front of a slug. These pressure drops are also listed in Table 2.

The difference between these two pressures, P1 and P2, for each case indicates the pressure drop across the slug body at low Froude numbers. At high Froude numbers, this difference still

includes the accelerational pressure loss, since the mixing zone is longer than that at lower Froude numbers. This can also be seen from the calculated accelerational pressure drop. At low Froude numbers, ΔP_a is smaller than P1, whilst at large Froude numbers, ΔP_a becomes larger than P1.

Pressure drops across the slug front (mixing zone) were found to be much larger than the pressure drops across the slug body (without the mixing region). This agrees with the experimental results of Dukler and Hubbard[6]. The calculated results of ΔP_a show that it is about 70% to 90% of the total pressure drop (P2).

It is also found that the pressure drop across the slug front decreases with an increase of the oil fraction. This is due to the apparent decrease in turbulence levels at the slug front with an increase in the oil concentration. It is also found that the pressure drop increases with increase in Froude number. A higher pressure drop within the slug indicates a larger energy loss there. This is associated with greater turbulence in the flow within the mixing zone.

Corrosion/Erosion Rate Measurements

The corrosion/erosion rates for the various test fluids, without any corrosion inhibitor present are given in Table 3, and Figures 13, 14, and 15. These show the change of probe reading with time for water, and oil-water mixtures of 20% oil and 80% water, and 40% oil and 60% water, respectively. The corrosion rate can be calculated by using the following equation:

$$\text{Corrosion Rate, mils/yr} = \frac{(\text{Probe dial change}) \times 5 \times 24 \times 365}{(\text{Measuring Period,hr}) \times 1000} \quad\text{....} \quad (5)$$

In each case it can be seen that the corrosion rate at the bottom of the pipe is always greater than that at the top. This is probably due to the shear stresses at the bottom being greater than those at the top as shown earlier. This has been further proven by recent experiments with full pipe flow using three compositions of synthetic seawater (saltwater, with viscosity of 1.3 times of pure water), mixture of 80% saltwater and 20% ARCO PAC 90 oil (this oil has a viscosity of 850 times of pure water), and mixture of 80% saltwater and 20% LVT-200 oil (with viscosity of 2.2 times of pure water). Two flow velocities of 0.5 and 1.8 m/sec under three CO_2 partial pressures of 25, 50, and 100 psig have been chosen in this test. The result of this experiment is shown in Table 4. Clearly we can see from Table 4 that the corrosion/erosion rates increase significantly with increasing CO_2 partial pressure. This may due to the increase of the amount of carbonic acid in the flow system.

The wall shear stresses in these flow conditions can be calculated. They change from 0.16 to 1.6 N/m^2 for fluid of saltwater only, from 0.3 to 2.9 N/m^2 for mixture of 80% saltwater and 20% LVT-200 oil, and from 4.4 to 16.0N/m^2 for mixture of 80% saltwater and 20% ARCO PAC 90 oil. The effect of the increase of wall shear stress on the corrosion/erosion rate can be seen in Table 4. For example, when the flow rate increases from 0.5 to 1.8 m/sec, the corrosion rates increase from 45 to 60 , 80 to 110, and 115 to 160 mils/year at system pressure of 25, 50, and 100 psig, respectively. The wall shear force may play an critical role in removing the corroded layer (which also serves as a protected film to prevent further corrosion) at the wall surface. This may explain why high corrosion rates can be measured in a slug mixing zone where maximum shear stress (coupled with high flow turbulency) can be orders of magnitude larger than for a full pipe flow. This indicates

that shear stress could be a very detrimental factor in the formation and persistence of corrosion inhibitor film at the wall surface.

Adding oil into the flow system can also increase the wall shear stress, which in turn increases the corrosion/erosion rate at the wall. This has also been shown in Table 3 where corrosion rate increases with increasing oil concentrations at all three Froude numbers. It can also be seen from Table 3 that the difference of these corrosion/erosion rates increase with increasing Froude numbers for all fluid compositions.

The corrosion rate at the bottom of the pipe increases sharply with an increase in Froude number, while the corrosion rate at the top decreases. This is also due to the substantial increase in wall shear at the bottom of the pipe and the flow turbulent intensity at these higher Froude numbers. The decrease at the top is due to the large amount of gas being entrained at the slug front and, thus, more gas exists near the top at the larger Froude numbers.

It is also noted that the corrosion rates measured are much higher than those predicted by usual single phase experiments (either by wheel tests or bubble tests) which usually only give about one-third to one-tenth of what is given in this experiment[19].

As the concentration of oil is increased, the corrosion rate at the bottom of the pipe increases substantially, whilst that at the top only changes slightly. For example, at a Froude number of 6, the corrosion rates at the bottom and at the top for water only are 81 and 75.2 mils/year (about 2 mm per year), respectively, but those for 15% water and 85% oil can reach 405 (about 1 cm per year) and 89.4 mils/year, respectively. This was not expected but could be due to the fact that erosion-corrosion, caused by the scouring action of the high shear forces, may play a significant role at these flow conditions rather than just corrosion alone. These corrosion rates are again at least an order of magnitude greater than those projected from the single phase data.

SUMMARY AND CONCLUSIONS

Based on results from the experimental measurements and visual observations, the following conclusions are made.

Void Fraction (or Liquid Holdup)

1. In this study the void fraction in the slug at the top of the pipe is always greater than that at the bottom. This indicates that gravity and buoyancy force are significant in slug flows in horizontal pipelines.
2. The flow tends to be more homogeneous in the mixing zone as the Froude number increases.
3. The amount of gas entrained increases with an increase in Froude number. The experimental results show good agreement with predictions using the empirical correlation of Gregory et al.[16]. However, the effect of pipe size on the liquid holdup in slug flow becomes significant for large Froude numbers, where different flow mechanisms are present.
4. An empirical correlation, similar to that of Gregory et al.[16], has been derived from the measured data. Better agreement with experimental results can be achieved using this correlation obtained in this test setup than using others from the literatures.
5. The amount of gas entrained decreases with the addition of the oil phase: the larger the oil concentration, the larger the liquid holdup.

Pressure Drops

1. The pressure drop across a slug body consists of the pressure drop due to the acceleration of liquid (or deceleration for a stationary slug) in the mixing zone and the frictional pressure drop after the mixing region. The former is much greater than the latter.
2. The frictional pressure drop across the slug front and within the slug body and the pressure drop due to the acceleration of liquid increase with an increase in the Froude number but decrease with an increase in oil concentration. The decrease of pressure drop comes mostly from the reduction of the degree of mixing in the slug front.
3. The measurements of pressure drop and the calculated results of pressure drop due to acceleration of liquid film indicate that the mixing length increases with increasing Froude numbers.

Wall Shear Stresses and Flow Turbulent Intensity near the Wall

1. The wall shear stress changes substantially across the front of the slug. The greatest changes occur at high Froude numbers.
2. The wall shear is always greatest at the bottom of the pipe and decreases towards the top.
3. Both the wall shear stress and turbulent intensity increase with an increase in Froude number.
4. Adding the oil phase into the flow system increases the wall shear stress but decreases the turbulent intensity of the flow.

Corrosion/Erosion Rates

1. The corrosion rates at the bottom of the pipe are always greater than those at the top. The corrosion rate at the bottom increases with an increase in Froude number, but the corrosion rates at the top decrease with an increase in Froude number.
2. An increase in the oil fraction increases the corrosion rate at the same Froude number.

NOMENCLATURE

English Letters

A	cross-sectional area
F, Fr	Froude number
g	acceleration due to gravity
H_L	liquid holdup
h_{eff}	effective height
P	pressure
ΔP_a	pressure drop due to acceleration of liquid film ahead of a slug front
V	velocity
x	mass picked up by the slug, shown in Equation (4)

Greek Letters

α	void fraction

Subscripts

eff	effective quantity
fe	liquid film region
G	gas phase
L	liquid phase
M	mixture
s	slug body
t	translational

REFERENCES

1. Jepson, W. P.: "Flow Characteristics in Horizontal Slugs," 3rd Int. Conf. on Multiphase Flow, The Hague, Netherlands (1987)187-197.

2. Jepson, W. P.: "Modelling the Transition to Slug Flow in Horizontal Conduit,". Can. J. Chem. Eng., V. 67,(October 1989) 731-740.

3. Choi, H. J. and Cepulis R. L.: "Inhibitor Film Persistence Measurement by Electrochemical Techniques," SPE Production Engineering, (November 1987) 325-329.

4. Ellison, B. T. and Wen, C. J., Am. Inst. Chem. Eng. Symp. Ser., Vol. 77 (1981) 161, cited from Sydberger, T. :"Flow Dependent Corrosion: Mechanisms, Damage Characteristics, and Control," Br. Corros. J., Vol. 22, No. 2 (1987) 83-89.

5. Green, A. S., Johnson, B. V., and Choi, H.:"Flow-Related Corrosion in Large-Diameter Multiphase Flowlines," SPE 20685 (1990) 677-684.

6. Mandhane, J. M., Gregory, G. A. and Aziz, K :"A Flow Pattern Map for Gas-Liquid Flow in Horizontal Pipes," Int. J. Multiphase Flow, Vol. 1 (1974) 537-553.

7. Lin, P. Y.:"Flow Regime Transitions in Horizontal Gas-Liquid Flow," University of Illinois, Ph. D. Thesis, (December 1984) 216.

8. Dukler, A. E. and Hubbard, M. G.:"A Model for Gas-Liquid Flow in Hori-zontal or Near Horizontal Tubes," Ind. Eng. Chem. Fund., Vol.14 (1975) 337-347.

9. Maron, D. M., Yacoub, N., and Brauner, N.:"New Thoughts on the Mechanism of Gas-Liquid Slug Flow," Letters in Heat and Mass Transfer, Vol. 9, No. 5 (1982 333-342.

10. Mercer, A. D.:"Test Methods for Corrosion Inhibitors," Br. Corros. J., Vol. 20, No. 2 (1985) 61-70.

11. Sun, J.:"Multiphase Slug Flow Characteristics and Their Effects on Corrosion in Pipelines", University of Illinois at Urbana-Champaign, Ph.D. Thesis, (May 1991) 178.

12. Newton, L. E., Advances in CO_2 Corrosion, Vol. 2, eds. P. A. Burke, A. I. Asphahani, and B. S. Wright (Houston, TX, Nace, 1984) 235-249.

13. Martin, R. L., Advances in CO_2 Corrosion, Vol. 2, eds. P. A. Burke, A. I. Asphahani, and B. S. Wright (Houston, TX, Nace, 1984) 250.

14. Mckenzie, M. and Vassie, P. R.:"Use of Weight Loss Coupons and Electrical Resistance Probes in Atmospheric Corrosion Tests," Br. Corros. J., Vol. 20, No. 3 (1985) 117-124.

15. Mckenzie, M. and Vassie, P. R.: "Use of Weight Loss Coupons and Electrical Resistance Probes in Atmospheric Corrosion Tests," Br. Corros. J., Vol. 20, No. 3 (1985) 117-124.

16. Chow, V. T. (1959). "Open Channel Hydraulics," McGraw-Hill, New York.

17. Gregory, G. A., Nicholson, M. K., and Aziz, K.: "Correlation of the Liquid Volume Fraction in the Slug for Horizontal Gas-Liquid Slug Flow," Int. J. Multi-phase Flow, Vol. 4 (1978) 33-39.

18. Kvernvold, O., Vindoy, V., Sontvedt, T., Saasen, A., and Selmer-Olsen, S.:"Velocity Distribution in Horizontal Slug Flow," Int. J. Multiphase Flow, Vol. 10, No. 4 (1984) 441-457.

19. Kolts, J., E. Buck, D. D. Erickson, and M. Achour (1990). "Corrosion Prediction and Design Considerations for Internal Corrosion in Continuously Inhibited Wet Gas Pipelines," paper provided by Conoco Inc.

Table 1 Void fraction distributions for different compositions of liquid at different Froude numbers at 25 cm within the slug (i.e. from the jump front) at 30 psia

Froude Number	Location*	Water Only	80% Water 20% Oil	60% Water 40% Oil
Fr = 6	1	.0304	.0016	0
	2	.077	.033	0
	3	.165	.036	0.008
	4	.216	.077	0.023
	5	.263	.163	0.072
Fr = 9	1	.036	.037	0.008
	2	.099	.040	0.050
	3	.251	.338	0.208
	4	.548	.435	0.368
	5	.640	.467	0.500
Fr = 12	1	.060	.080	0
	2	.112	.120	0.068
	3	.354	.456	0.300
	4	.502	.600	0.542
	5	.604	.653	0.547

* Dimensionless distances from the bottom of the pipe, 1 = .054,
2 = .225, 3 = .475, 4 = .725, 5 = .947.

Table 2 Pressure drops across a stationary slug.

Fr and Pressure Tap Locations	Water only	20% Oil and 80% Water	40% Oil and 60% Water	Oil only
Fr = 6, P1*	25.80	22.50	20.60	18.30
P2*	30.40	24.00	21.10	18.50
ΔP_a	19.22	18.65	18.02	16.22
Fr = 9, P1*	54.40	43.60	40.80	N/A
P2*	61.62	51.50	48.30	N/A
ΔP_a	44.73	41.02	39.65	N/A
Fr = 12, P1*	70.50	47.30	46.70	N/A
P2*	102.3	89.10	84.70	N/A
ΔP_a	80.8	74.20	70.05	N/A

P1 = Pressure tap at 30 cm within the stationary slug.
P2 = Pressure tap at 60 cm wihtin the slug.
N/A = Not available

Table 3 Corrosion/Erosion rate measurements for different fluid composition at various Froude numbers at system pressure of 30 psia.

Fluid Composition	Froude Number	Top*	Bottom*
Water Only	6	75.19	81.40
	9	47.82	154.4
	12	37.23	199.3
90% Water and 10% Oil	11.8	62.78	188.34
80% Water and 20% Oil	5.8	87.24	159.1
	8.9	81.40	145.6
	12	78.84	240.9
60% Water and 40% Oil	6	103.4	213.2
	9	71.18	152.9
	11	67.89	298.9
	12	57.31	354.8
15% Water and 85% Oil	6	89.43	405.2

*The unit is Mils/year, 1 probe reading change in 120 min
= 21.9 Mils/year

Table 4 Corrosion/erosion rate measurement (in mils/year) for different fluid compositions at full pipe flow with various flow rates.

System Pressure (psig)/Flow Velocity (m/s)	Salt Water Only	80% Saltwater & 20 % LVT-200 Oil	80% Saltwater & 20 % ARCO PAC 90 Oil
25/0.5	45	48	65
25/1.8	60	63	97
50/0.5	80	112	120
50/1.8	110	126	150
100/0.5	115	135	168
100/1.8	160	170	200
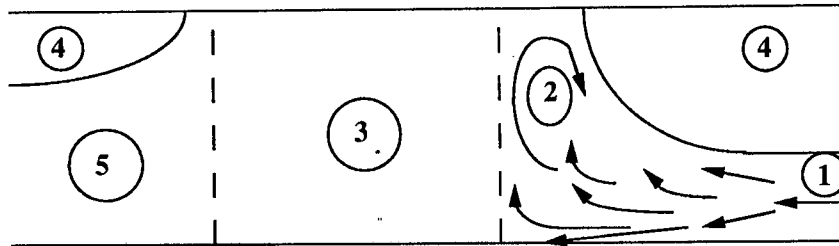
1 - Liquid Film
2 - Mixing Zone
3 - Slug Body
4 - Gas Bubble Zone
5 - Slug Tail

Figure 1   Idealized Slug Unit
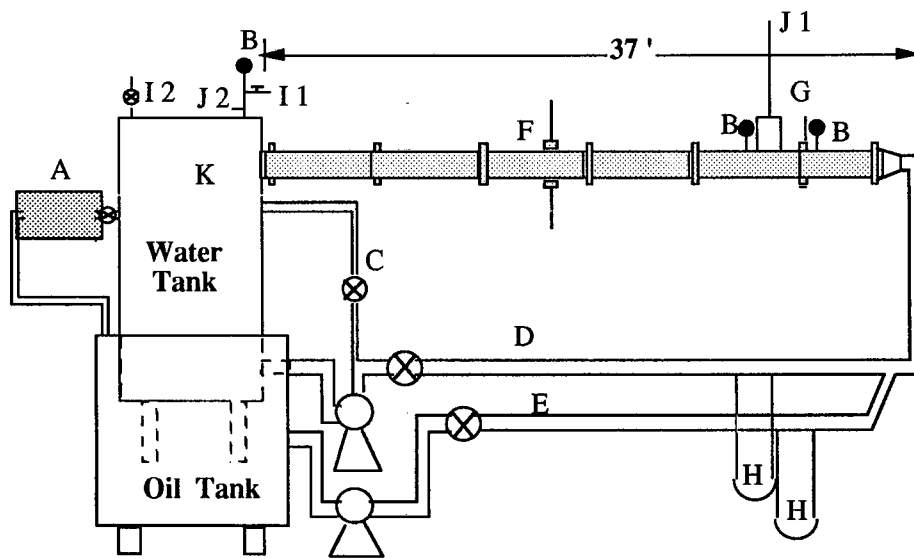
A. Water/Oil Separator
B. Pressure Guages
C. Water Recycle
D. Water Feed - 3" PVC
E. Oil Feed - 3" PVC
F. Test Section - 4" Plexiglass

G. Flow Height Control Gate
H. Orifice Plate Manometers
I. Pressure Relief Valve
J. CO2 Feed Line
K. Liquid/Gas Separator

Figure 2   Layout of the experimental system

Overall length - 6 ft.

A

B

E

Direction of Flow

O E

E

D D D D

C

B

A. Resistance Probes
B. Ball Valves
C. Sample Tube
D. Pressure Tappings
E. Shear Probe Mountings

A
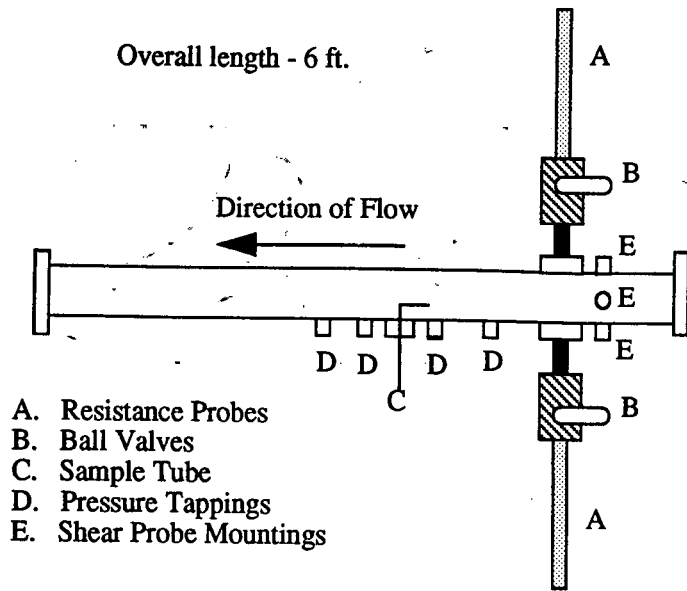
Figure 3   Layout of the test section

$F_1 = 1-1.7$ Undular jump

$F_1 = 1.7-2.5$ Weak jump

Oscillating jet

Roller

$F_1 = 2.5-4.5$ Oscillating jump

$F_1 = 4.5-9.0$ Steady jump

$F_1 > 9.0$ Strong jump
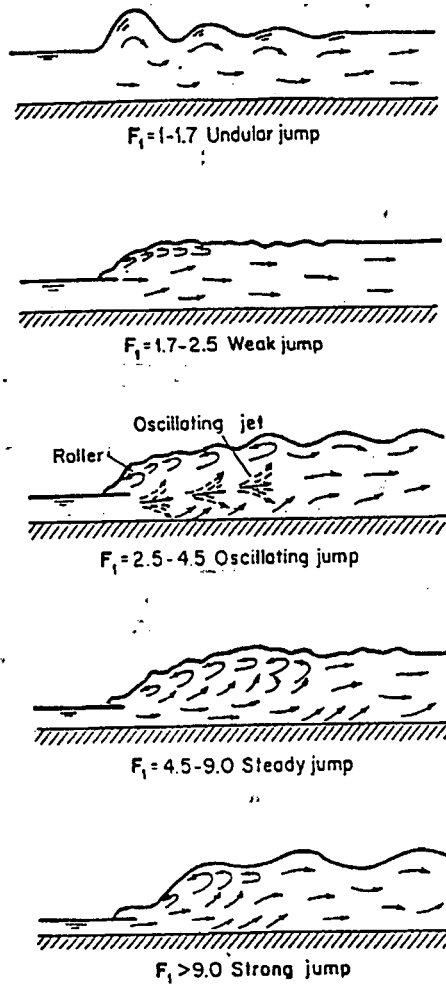
Figure 4   Strength of hydraulic jump as function of Froude numbers. [16]
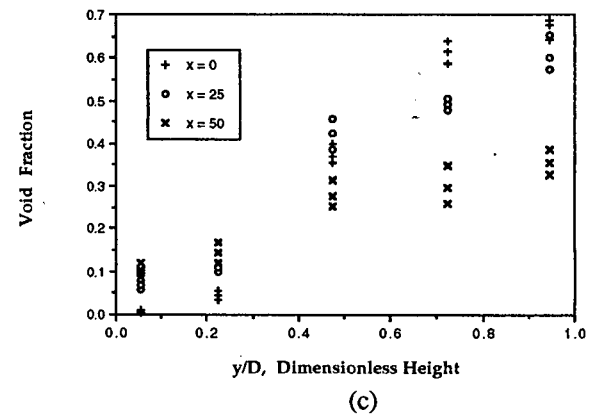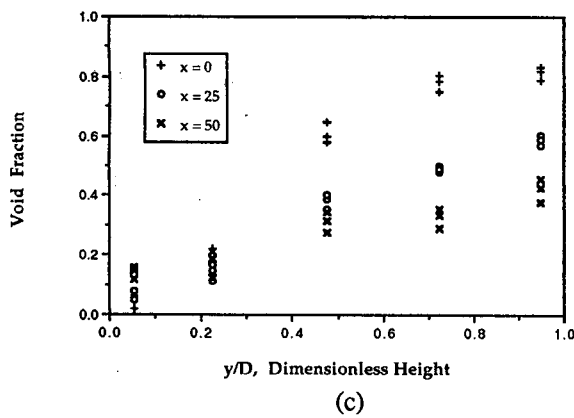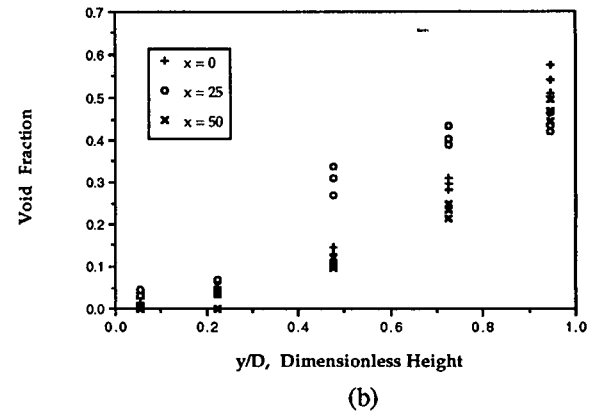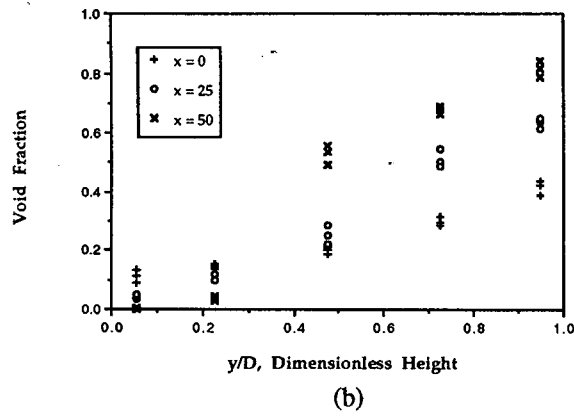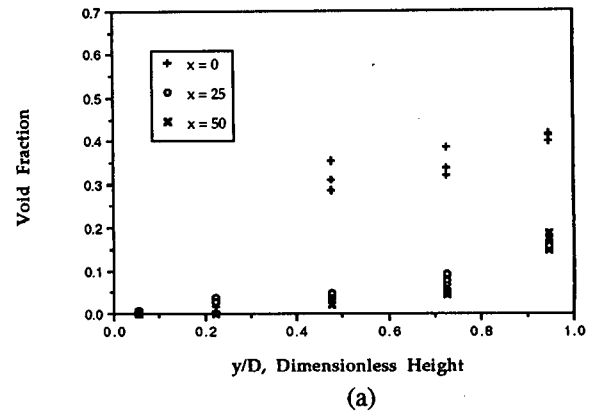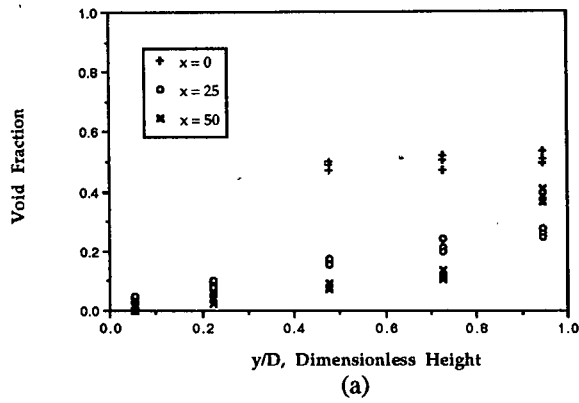
Figure 5   Void fraction distribution of water-CO_2 system at Frouder numbers of (a) 6, (b) 9, and (c) 12. System pressure is 30 psia.

Figure 6   Void fraction distribution of flow system of an oil-water mixture of 20% oil and 80% water with CO_2 at Froude numbers of (a) 6, (b) 9, and (c) 12. System pressure is 30psia.
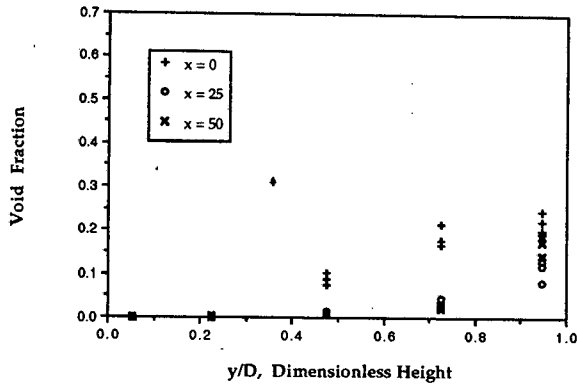
(a)
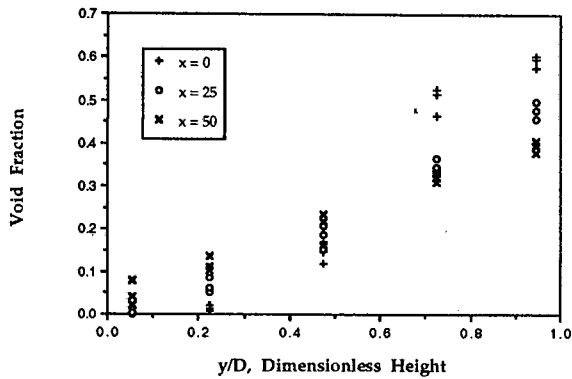
(b)
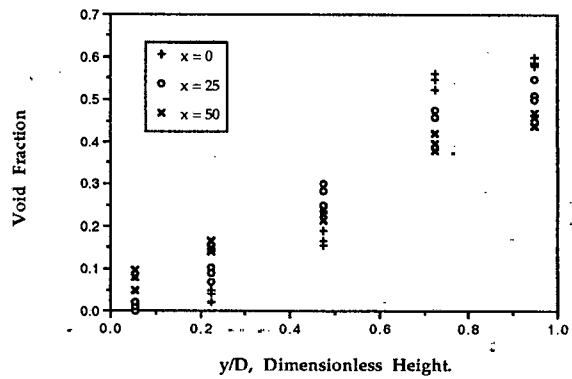
(c)

Figure 7   Void fraction distribution of flow system of an
oil-water mixture of 40% oil and 60% water with
CO_2 at Froude numbers of (a) 6, (b) 9, and (c) 12.
System pressure is 30psia.
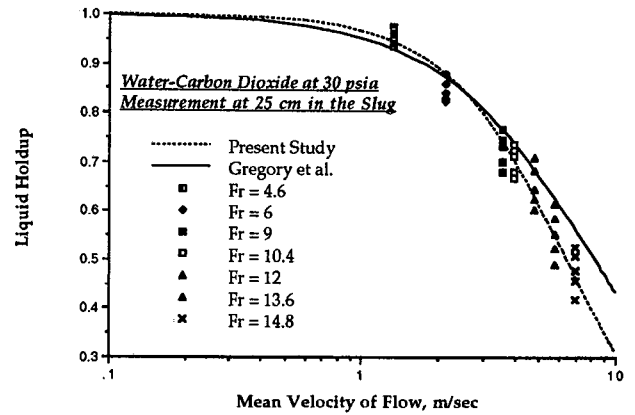
Figure 8   Comparison between the measured average liquid
holdup at various Froude numbers and correlation
from Gregory et al.[17].
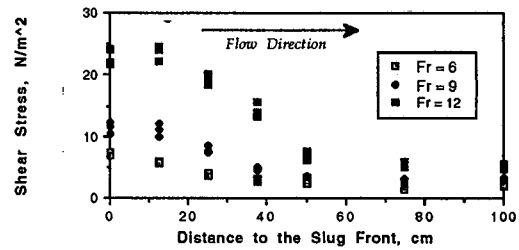
(a)
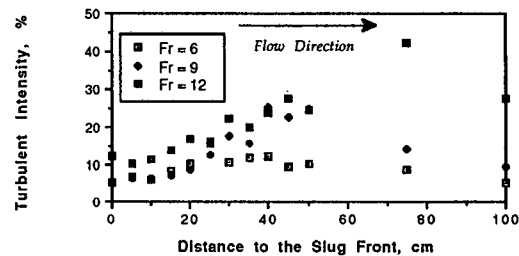
(b)

Figure 9   Mean wall shear stress (a) and turbulent inten-
sity (b) for water only at system pressure of
30 psia.
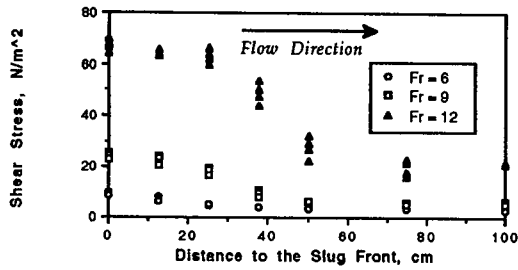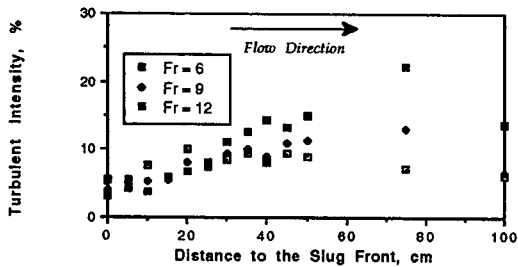
Figure 10 Mean wall shear stress (a) and turbulent intensity (b) for oil-water mixture of 20% oil and 80% water at system pressure of 30 psia.

Figure 11 Mean wall shear stress (a) and turbulent intensity (b) for oil-water mixture of 40% oil and 60% water at system pressure of 30 psia.
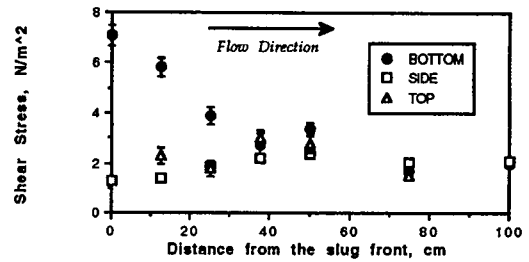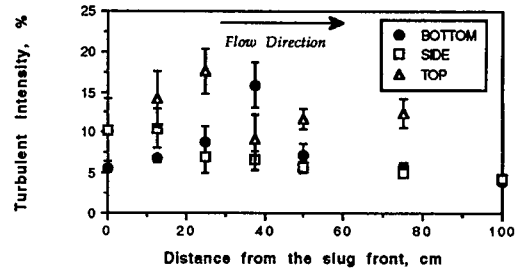
Figure 12 Wall mean shear (a) and turbulent intensity (b) for water only at bottom, side, and top of the pipe at 15 psia and Froude number 6.
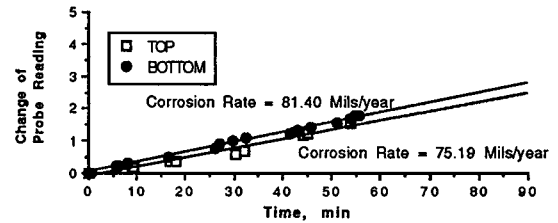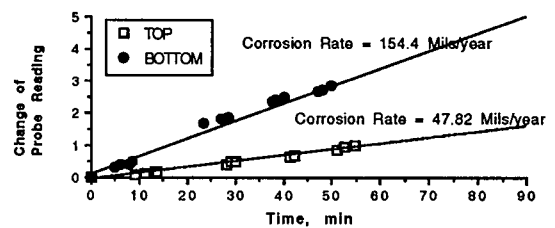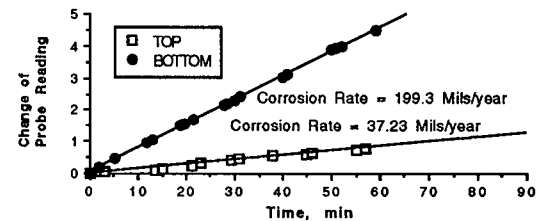
Figure 13 Corrosion/Erosion rate measurement at 30 psia for runs with water only at Fr = (a) 6, (b) 9, and (c) 12. 1 probe reading change in 120 min.= 21.9 Mils/year

227
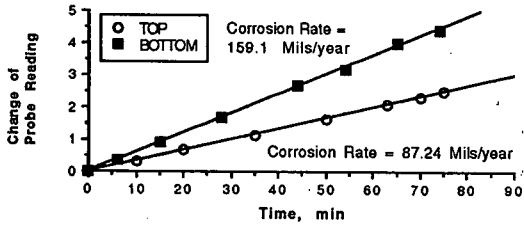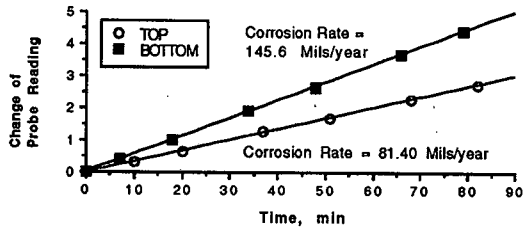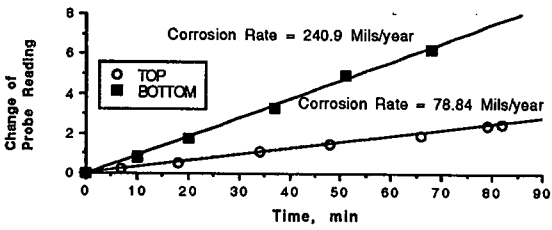
Figure 14 Corrosion/Erosion rate measurement at 30 psia for mixture of 80% water and 20% oil at Fr = (a) 6, (b) 9, and (c) 12.   1 probe reading change in 120 min. = 21.9 Mils/year
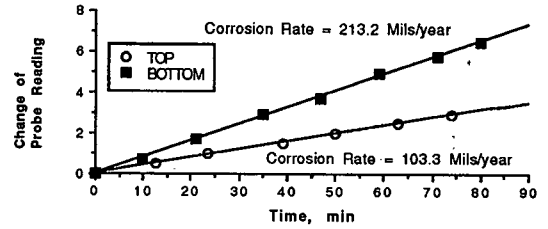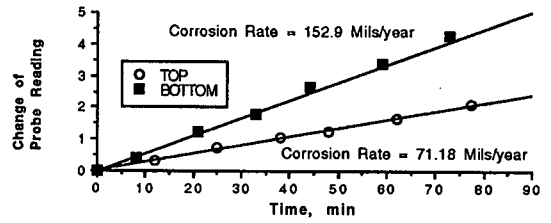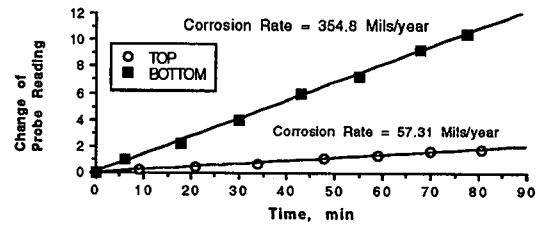
Figure 15 Corrosion/Erosion rate measurement at 30 psia for mixture of 60% water and 40% oil at Fr = (a) 6, (b) 9, and (c) 12. 1 probe reading change in 120 min. = 21.9 Mils/year